Direct Write Optical Waveguide Fabrication in organic films using a Heidelberg Laser Writer

Ryan Moss
Electrical and Microelectronic Engineering Department
Rochester Institute of Technology
Rochester NY, United States

Stefan Preble Principle Advisor
Nanophotonics Group
Rochester Institute of Technology
Rochester NY, United States

***Abstract*— Fabrication and characterization of mr-DWL photoresist buried channel waveguides on glass is carried out using the Heidelberg DWL 66+ (a laser direct write system). Waveguides are formed of mr-DWL-5 on glass with a spun on cladding material Norland Optical Adhesive-65(NOA- 65). The optical waveguides are successfully coupled at 650nm, and resonance structures tested at 710nm. Ring resonators with nominal spacing of .9um and a radius of 350um have an approximate quality factor of 71k .**

Keywords—waveguide; direct write; negative resist

I. Introduction

Polymer material as a waveguide is popular due to simplicity in fabrication, its general cost and its ability to be formed onto any surface. SU-8 photoresist material has been a highly investigated waveguide material. It is a negative tone epoxy photoresist with high contrast, and high optical transparency in the visible and near IR regions. The Heidelberg DWL 66+ is designed for 405nm wavelength and has 2 write heads designed for .8um resolution and 2um respectively. mr-DWL-5 is a direct write version of SU-8 photoresist that is expected to have similar properties but is chemically active at the required wavelength for

II. Theory

A. *Waveguide*

A buried channel device has characteristics governed by its cross-sectional geometry.

There are two critical angles associated with the waveguide (one for each material boundary). The critical angles are defined by

$$\theta_{c1} = \sin^{-1}\frac{n_c}{n_w} \qquad \theta_{c2} = \sin^{-1}\frac{n_s}{n_w} \tag{1}$$

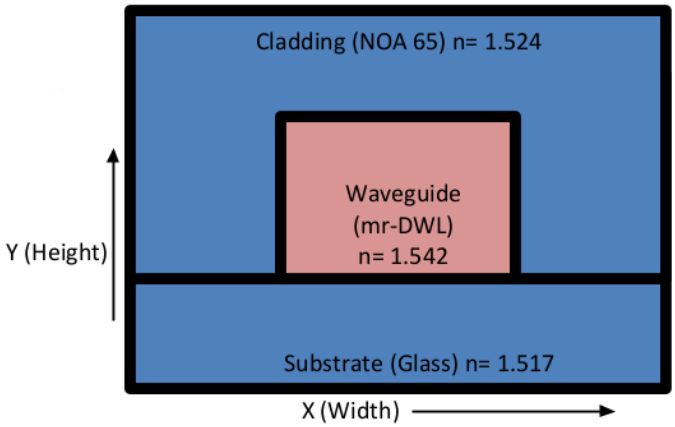

Figure 1: Waveguide cross-section

n_w, n_c and n_s are the index of refraction for the waveguide(1.542), cladding(1.524) and the substrate(1.50) respectively. Therefore the angles of total internal reflection are 79.7° for the substrate and 81.2° for the cladding. Angles greater than the critical angle are constrained within it, this is the basis for a waveguide's use as an optical interconnect. The critical angle is also used to calculate the acceptance angle, the angle at which light needs to be incident to enter the guide.

While traveling through the guide the transverse portion of the wave (within the cross-section) interferes with itself forming waveguide modes. The optical modes are a function of the difference in the index and the height and width of the waveguide. The generation of these modes is due to the interference of the light after rebounding due to total internal reflection in the waveguide. The transverse and longitudinal portions of the wave are calculated

$$k_{x,y} = \frac{n_w\omega}{c}\cos\theta \qquad k_z = \frac{n_w\omega}{c}\sin\theta \tag{2}$$

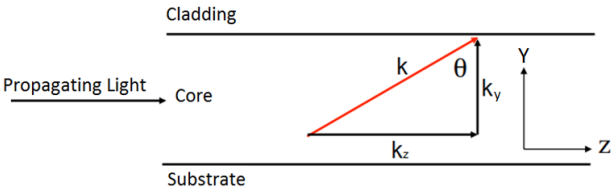

Figure 2: Side view of a beam through the waveguide

Waveguide modes occur when the phase change in a round trip transverse path in the waveguide is a multiple of 2π. The phase change is a total of the phase changes at the boundaries and the phase change over the cross-sectional geometry. The rectangular shape of the guides cannot be solved analytically.

B. Simulation

The solutions to the electric field optical modes within the waveguide must be solved numerically. Simulations in this paper are done using COMSOL's optical tools. COMSOL uses beam approximation method. Which uses a solution to the spatial Helmholtz equation, which uses the wavenumber k_o in vacuum, the indices of the materials n, and the electric field.

$$\left(\nabla^2 + k_o{}^2 n^2\right)\vec{E}(x,y) = 0 \tag{3}$$

This is then solved for the surface normal electric field in all space (E(x,y)) for a cross section of the waveguide.

The device cross-section is modeled at 1.2um width, the layout width of design, and a height of 1.18um, the expected thickness at 4000rpm spin speed. This creates a cross section which is relatively square, which is desired to minimize multimode behavior.

The indices of 1.542, 1.524 and 1.517 are used for SU-8, NOA-65 and borosilicate glass respectively. For 650nm incident light the electric field magnitude is plotted in figure 3. The simulation shows mismatch of substrate and cladding material draws the propagating light away from the substrate and into the cladding. The degree of electric field outside the boundary of the waveguide predicts a high expected attenuation.

Near the completion of the project a scanning electron microscope revealed shorter and wider device geometry than expected (see IV. Results). A simulation with these device geometries is then done. The shorter device geometry makes the resonant mode extend further outside the waveguide creating additional loss. In addition the wider device geometry suppresses the T_m mode. Finally the larger base in comparison to the top negates part of the index mismatching drawing more of the light into the waveguide.

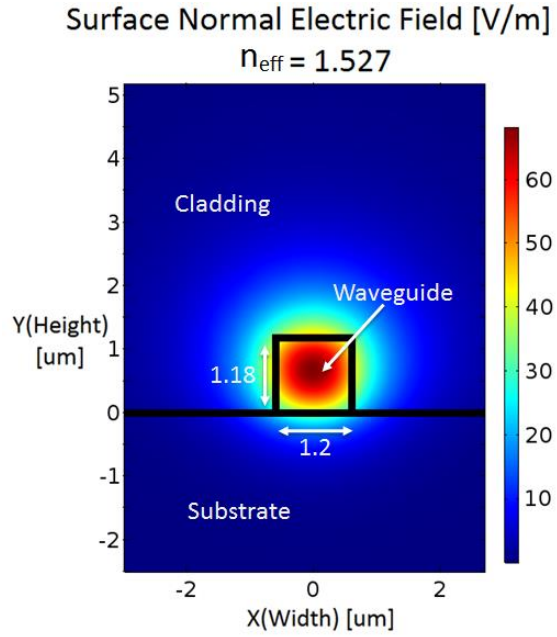

Figure 3: COMSOL simulation optical resonance mode. This 1st order mode has an effective index of 1.527. The T_e and T_m modes have similar propagation.

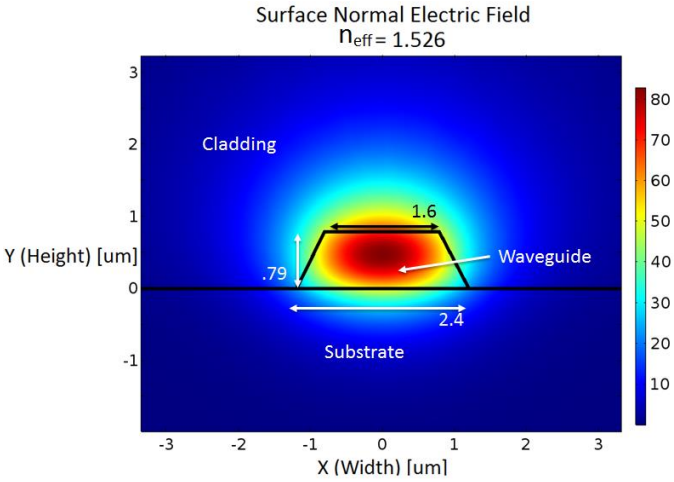

Figure 4: Simulation using the dimensional results for the Scanning Electron Microscope pictures. The T_e mode is enhanced by the wider base while the T_m mode is suppressed.

C. Coupling between Waveguides and Ring Resonators

The final stage of the project was creating a ring resonator. A ring resonator is formed by coupling light into a waveguide that loops back on itself. Resonance occurs when the length of the loop is a multiple of the wavelength inside the guide. The resonator is defined by its quality factor which is a measure of the energy lost per cycle.

$$Q = \frac{E_o}{\Delta E} 2\pi \tag{4}$$

This project will be defining the quality via resonance bandwidth which can be calculated using the wavelength and the full width at half maximum of the peak.

$$Q = \frac{\lambda_o}{\Delta\lambda} \quad (5)$$

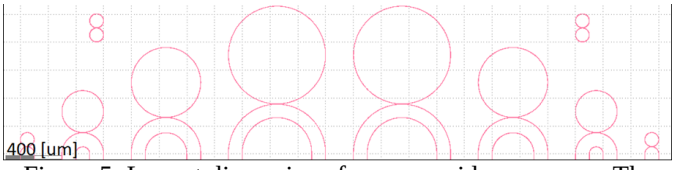

Figure 5: Layout dimensions for waveguide exposure. The gap between the ring resonator and the directly coupled waveguide is varied from .8um to 1.2um. All waveguides have a layout width of 1.2um.

In order to couple into this loop a waveguide is placed adjacent. The overlap of the electric field from the waveguide mode of the adjacent ring waveguide mode causes photons to transfer into the ring waveguide. The longer the overlapping section the more photons that will be transferred, increasing the coupling. With a resonator however greater coupling can cause suppression of the mode as this coupling defines the device instead of the ring shape. Photons no longer stay within the resonator and transfer freely between the parallel waveguides. Finding a balance of entry and exit from the ring resonator is essential.

III. Process

Fabrication consists of creating waveguides with a basic coat, exposure and development. Optical properties are then solidified by coating a cladding material of the correct index. Then scribe to the desired waveguide length. Exact procedure for waveguides measured is as follows.

1. Oxygen Plasma Surface Treatment.
2. Coat mr-DWL dilution. 40mL/40mL dilution of mr-DWL-5 and SU-8 Thinner. The base spin recipe

Spin Speed [rpm]	Thickness [um]
3000	1.47
4000	1.18
5000	1.01

Table 1: Measured coat thickness of mr-DWL dilution with various spin speeds.

   Post application bake is done on a hot plate at 65°C for 4 minutes.
3. Negative resist exposure on the Heidelberg. Key parameters used are 60% intensity and 200mW power.
4. Post Exposure Bake 1 minute at 65°C followed by 3 minutes at 95°C
5. Development PGMEA chemistry bath no agitation 3.5 minutes followed by bath rinses in IPA and water.
6. Spin Coat cladding material NOA-65. Spin Speed 3000rpm.
7. Cure cladding material using flood exposure with final dose 4.5 J/cm^2
8. Scribe and Cleave to devices. Polishing to uniform planarity has exhibited issues with delamination of the film stack is therefore not used.

IV. Results

A scanning electron microscope was used to look at the cross section of finished waveguides.

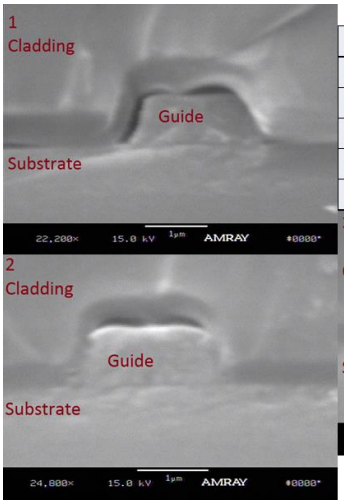

SEM Measurements [um]			
	1	2	3
Top	1.4	1.8	1.64
Bottom	2.4	2.4	2.5
Average Width	1.9	2.1	1.93
Average Height	0.8	0.8	0.79

Figure 6: SEM measurements of waveguide cross-section. Cross-section widths are larger than nominal and the height is less than expected at a spin speed of 5000rp. These were spun at 3000rpm.

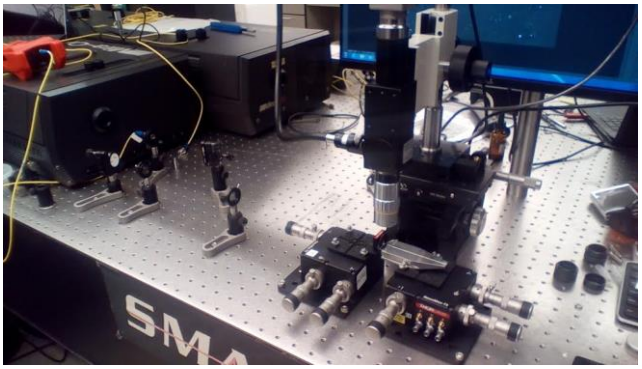

Figure 7: Optical Testing setup. A titanium Sapphire laser coupled into the waveguides and observed using an optical microscope. Alignment of the beam and sample is achieved using adjustments in x,y and z.

Waveguide testing was accomplished by aligning a focused laser source onto the waveguide (direct focusing). Initial coupling was done using a collimated laser beam from a fisher scientific visual fault locator with output power of 1mW and a typical wavelength of 650nm. Coupling is evident by the light escaping from the waveguide into a microscope optical field

seen using a digital camera (Pco.pixelfly) and analyzed using Camware v3.14. Although no output intensity was measured, visual analysis can reveal basic premises. Larger radii curves on waveguides have lower losses. Losses are mostly seen at the smallest curvature (radius-50um). Light transfer between adjacent waveguides is demonstrated.

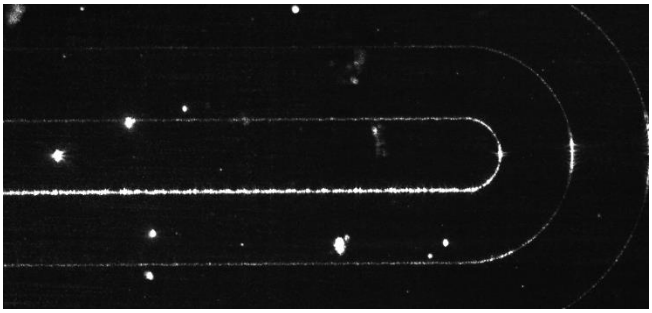

Figure 6: Coupled waveguide with 50um bend. Visual loss is easily seen as the light transitions from the bottom to the top.

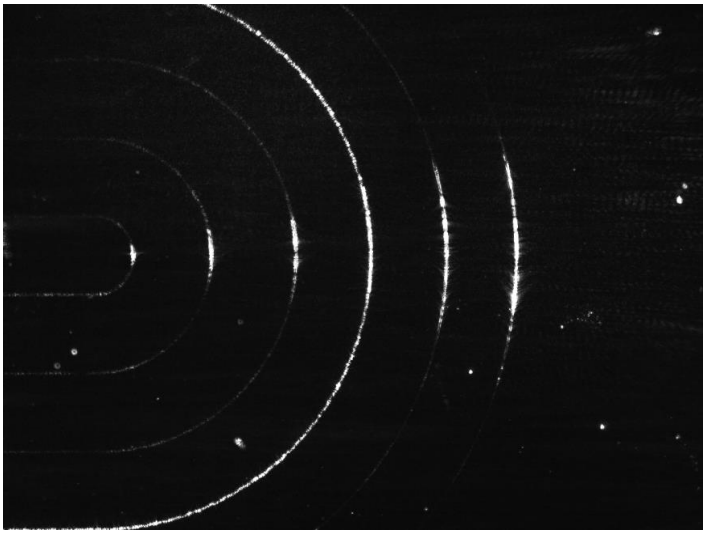

Figure 8: Coupled waveguide with 350um bend. Visual loss cannot be seen through the curve.

Finally an M Squared continuous titanium sapphire laser was used in conjunction with a wavelength meter to tune the crystal cavity to vary the wavelength slowly in order to observe the quality factor of a coupled resonator. The visual intensity was observed and FWHM was approximated for the ring resonator. At 710nm the FWHM was approximately .01nm yielding a quality factor of 71k using equation 5.

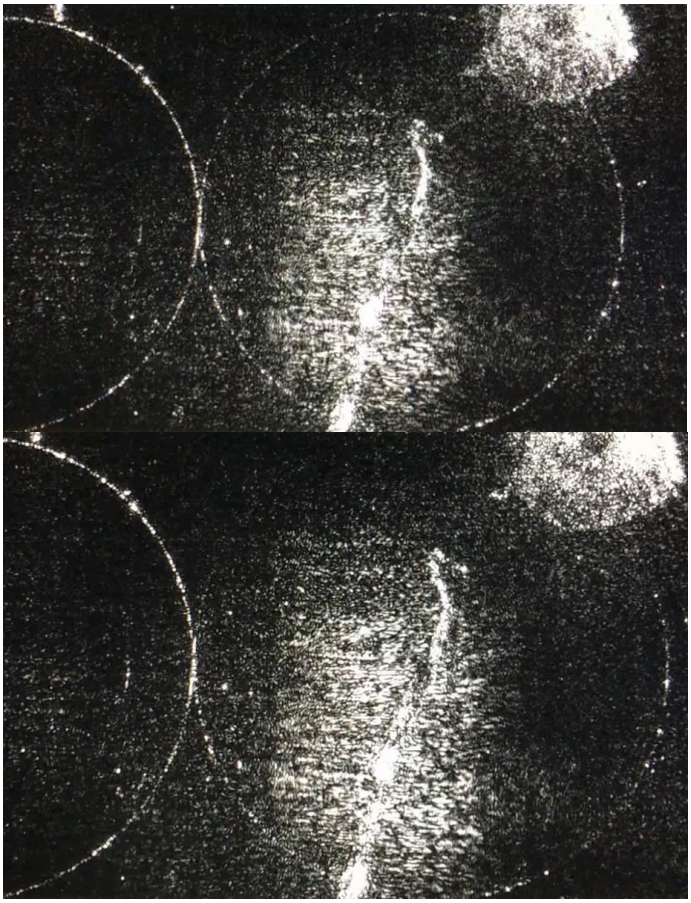

Figure 9: Coupled ring resonator structures. When the wavelength of light is varied the ring resonator exhibits resonance with visual intensity. At top the ring is at resonance while below the ring is weakly coupled.

V. Conclusions

The Heidelberg Laser writer is capable of creating optical waveguides cheaply and quickly. Currently the process needs optimization to improve losses and create additional types of devices. However this process has been shown to create functional waveguides on a glass substrate and create a ring resonator structure with an approximate quality factor of 71k.

VI. References

[1] S. Keller, G. Blagoi, M. Lillemose, D. Haefliger, and A. Boisen,"Processing of thin SU-8 films,"J. Micromech. Microeng., vol. 18, no.12, 125020, Nov. 2008 J. Clerk Maxwell, A Treatise on Electricity and Magnetism, 3rd ed., vol. 2. Oxford: Clarendon, 1892, pp.68–73.

[2] MicroChem Nano SU-8 2000 Process Sheet.